Binuclear Diphosphine-Bridged Iridium Complexes as Models for the Catalytic Hydrogenation of Alkynes in the Presence of Two Metal Centers. The Structure of $[Ir_2Cl_2(CH_3O_2CC{=}CHCO_2CH_3)_2(CO)_2(DPM)_2]$, a Product of Alkyne Insertions into Two Ir–H Bonds

Bruce R. Sutherland and Martin Cowie*

Department of Chemistry, The University of Alberta, Edmonton, Alberta, Canada T6G 2G2

Received November 6, 1984

The reactions of *trans*-$[IrCl(CO)(DPM)]_2$ (1) and $[Ir_2(CO)_2(\mu\text{-}Cl)(DPM)_2][BF_4]$ (2) (DPM = bis(diphenylphosphino)methane) with H_2 and the subsequent reactions of the dihydride products with dimethyl acetylenedicarboxylate (DMA) are reported. Compound 1 reacts with H_2 yielding $[Ir_2(H)_2Cl_2(CO)_2(DPM)_2]$ (3) in which the hydrido ligands are mutually cis on adjacent metals. This product reacts with 1 equiv of DMA to give $[Ir_2HCl_2(CH_3O_2CC{=}CHCO_2CH_3)(CO)_2(DPM)_2]$ (6) in which alkyne insertion into only one of the Ir–H bonds has occurred. Reaction of 2 with H_2 yields $[Ir_2(H)_4Cl(CO)_2(DPM)_2][BF_4]$ (4), and H_2 loss from this tetrahydride species yields $[Ir_2(H)_2(CO)_2(\mu\text{-}Cl)(DPM)_2][BF_4]$ (5), in which the two hydride ligands do not seem to be mutually cis. Compound 5 can also be generated from 3 by chloride ion abstraction using $AgBF_4$. Compound 5 reacts with a twofold excess of DMA in CH_2Cl_2 to yield $[Ir_2Cl_2(CH_3O_2CC{=}CHCO_2CH_3)_2(CO)_2(DPM)_2]$ (7) as the major product. Alkyne insertion into both Ir–H bonds has occurred, and the additional chloride ion seems to come from the solvent. Compound 7 crystallizes in the space group $P\bar{1}$ with a = 15.978 (2) Å, b = 20.460 (5) Å, c = 21.494 (2) Å, α = 107.86 (2)°, β = 90.46 (2)°, γ = 106.17 (2)°, and Z = 4. The structure, which confirms that alkyne insertion into each of the Ir–H bonds of the precursor has occurred, has refined to R = 0.061 and R_w = 0.090 based on 11275 observations and 545 parameters varied.

Introduction

Much of the present understanding of the mechanisms of homogeneous hydrogenation of unsaturated organic substrates comes from studies on mononuclear rhodium–phosphine complexes.[1] More recent studies have centered on the use of complexes containing more than one metal center as catalysts because of the potentially new modes of reactivity not available with mononuclear systems.[2,3] The functions of the different metal centers in these polynuclear complexes is especially intriguing. Reports of alkyne hydrogenation under mild conditions by the binuclear complexes $[Rh_2(CO)_2(\mu\text{-}Cl)(DPM)_2][BPh_4]$,[4] $[Rh_2(CO)_2(DPM)_2]$,[5] and $[Rh_2Cl_2(\mu\text{-}CO)(DPM)_2]$[6] caused us to question how the two metal centers in these complexes were involved in the catalysis; although it was attractive to consider that both metals were participating, perhaps in a cooperative manner, it was not clear from the studies reported that this was the case.

We have recently been studying binuclear, DPM-bridged complexes of iridium as models for multicenter metal catalysts[7-9] and decided to expand these studies to include alkyne hydrogenation. It was felt that with iridium we might be able to isolate complexes which would model intermediates in the rhodium-catalyzed reactions and by so doing we might gain an insight into these reactions and in particular gain some understanding of how the two adjacent metal centers functioned in catalysis; with the rhodium complexes no intermediates had apparently been observed.[4-6] Herein we report the initial results of this study.

Experimental Section

All solvents were appropriately dried and distilled prior to use and were stored under dinitrogen. Reactions were performed under standard Schlenk conditions using dinitrogen which had been previously passed through columns containing Ridox and 4A molecular sieves to remove traces of oxygen and water, respectively. Hydrated iridium(III) chloride was obtained from Johnson-Matthey and bis(diphenylphosphino)methane (DPM) was purchased from Strem Chemicals. Carbon monoxide was obtained from Matheson and used as received. *trans*-$[IrCl(CO)(DPM)]_2$ (1) and $[Ir_2(CO)_2(\mu\text{-}Cl)(DPM)_2][BF_4]$ (2) were prepared by the previously reported procedures.[7] Variable-temperature $^{31}P\{^1H\}$ NMR spectra were run on a Bruker HFX-90 spectrometer with Fourier transform capability operating at 36.43 MHz. The spectra were measured with an external acetone-d_6 lock, and chemical shifts were referenced to 85% H_3PO_4. ^1H NMR spectra were run on a Bruker WH-400 spectrometer unless otherwise stated. Infrared spectra were run on a Nicolet 7199 Fourier transform interferometer either as solids in Nujol mulls on KBr plates or as solutions in NaCl cells with 0.5-mm window path lengths. Analyses were performed by the microanalytical service within the department.

Preparation of Compounds. (a) $[Ir_2(H)_2Cl_2(CO)_2(DPM)_2]$ (3). An atmosphere of hydrogen was placed over a solution of *trans*-$[IrCl(CO)(DPM)]_2$ (1) (200 mg, 0.156 mmol) in 10 mL of CH_2Cl_2, and the mixture was stirred for 15 min, during which time the color changed from dark purple to light yellow. The solution was concentrated to a volume of 5 mL under hydrogen, and 30 mL of hexanes was added resulting in the precipitation of a pale yellow powder. The solid was collected and dried under a stream of hydrogen. Recrystallization from toluene/hexanes yielded 3, with 1 equiv of toluene of crystallization, as a colorless microcrystalline solid in 90% yield. Compound 3 was determined to

(1) James, B. R. "Homogeneous Hydrogenation"; Wiley: New York, 1974.
(2) Fryzuk, M. D.; Jones, T.; Einstein, F. W. B. *Organometallics* **1984**, *3*, 185.
(3) Burch, R. R.; Shusterman, A. J.; Muetterties, E. L.; Teller, R. G.; Williams, J. M. *J. Am. Chem. Soc.* **1983**, *105*, 3546.
(4) Sanger, A. R. *Prepr.—Can. Symp. Catal.* **1979**, *6th*, 37.
(5) Kubiak, C. P.; Woodcock, C.; Eisenberg, R. *Inorg. Chem.* **1982**, *21*, 2119.
(6) Cowie, M.; Southern, T. G. *Inorg. Chem.* **1982**, *21*, 246.
(7) Cowie, M.; Sutherland, B. R. *Inorg. Chem.* **1984**, *23*, 2324.
(8) Cowie, M.; Sutherland, B. R., *Organometallics* **1985**, *4*, 1637.
(9) Cowie, M.; Sutherland, B. R., submitted for publication.

0276-7333/85/2304-1801$01.50/0 © 1985 American Chemical Society

Table I. Spectral Data for the Compounds[a]

compound	infrared cm^{-1}		NMR	
	solid[b]	solution[c]	$^{31}P\{^1H\}$ δ[d]	^1H δ
$[Ir_2(H)_2Cl_2(CO)_2(DPM)_2]$ (3)	2012 (vs), 1972 (st),[e] 2091 (m), 2222 (w)[f]	2009 (st, br), 1971 (m, br),[e] 2073 (w, br), 2098 (sh, br), 2232 (w)[f]	−1.4, −8.6 (m), −5.2 (s),[i,k] −7.6 (m)[j]	7.6–7.1 (m, 40 H), 5.0 (br, 4 H), −5.76 (t, $^2J_{P-H}$ = 14.4 Hz), −15.10 (t, $^2J_{P-H}$ = 14.4 Hz),[i] −14.86 (t, $^2J_{P-H}$ = 12.5 Hz)[k]
$[Ir_2(H)_4Cl(CO)_2(DPM)_2][BF_4]$ (4)		2038 (st), 2073 (vs),[e] 1964 (w), 2147 (m), 2221 (w)[f]	−9.6 (m)	7.7–7.2 (m, 40 H), 5.04 (m, 2 H), 4.97 (m, 2 H), −10.00 (br, 1 H), −14.02 (br, 1 H), −14.46 (br, 1 H), −16.59 (t, 1 H, $^2J_{P-H}$ = 11.1 Hz)
$[Ir_2(H)_2(CO)_2(\mu\text{-}Cl)(DPM)_2][BF_4]$ (5)	1934 (vs),[e] 2067 (st)[f]		−1.3 (s)	7.55–7.34 (m, 40 H), 4.17 (s, 4 H), −13.50 (br t, 2 H)
$[Ir_2(H)(CH_3O_2CC{=}CHCO_2CH_3)Cl_2(CO)_2(DPM)_2]$ (6)	1982 (vs),[e] 2131 (w),[e] 1712 (st),[g] 1623 (w)[h]	1987 (vs), 2004 (vs),[e] 2148 (w)[f]	−2.8, −16.5 (m)	7.05–7.81 (m, 40 H), 5.19 (m, 2 H), 4.47 (m, 2 H), 3.85 (s, 1 H), 3.21 (s, 3 H), 2.97 (s, 3 H), −8.89 (t, 1 H)
$[Ir_2(CH_3O_2CC{=}CHCO_2CH_3)_2Cl_2(CO)_2(DPM)_2]$ (7)	1987 (vs), 1947 (m),[e] 1706 (vs),[g] 1582 (m)[h]	2002 (st), 1963 (m)[e]	−12.5, −16.5 (m)	7.43–6.92 (m, 40 H), 5.74 (m, 2 H), 4.81 (m, 2 H), 4.49 (s, 1 H), 4.75 (s, 1 H), 3.19 (s, 3 H), 3.28 (s, 3 H), 3.46 (s, 3 H), 3.48 (s, 3 H)

[a] Abbreviations used: st = strong, vs = very strong, med = medium, w = weak, sh = shoulder, s = singlet, m = multiplet, br = broad, t = triplet. [b] Nujol mull. [c] CH_2Cl_2 solution. [d] Vs. 85% H_3PO_4. [e] ν(CO). [f] ν(Ir–H). [g] ν(C=O) of CO_2CH_3. [h] ν(C=C). [i] −40 °C. [j] −100 °C. [k] Due to an additional product; see text.

be nonconducting in CH_2Cl_2 solutions ($\Lambda(10^{-3}$ M) $\leq 0.5\ \Omega^{-1}\ cm^2\ mol^{-1}$) but in nitromethane $\Lambda(10^{-3}$ M) = 61.1 $\Omega^{-1}\ cm^2\ mol^{-1}$.[10] Spectroscopic parameters for this and all subsequent compounds are given in Table I. Anal. Calcd for $Ir_2Cl_2P_4O_2C_{59}H_{54}$: C, 51.57; H, 3.96. Found: C, 51.64; H, 4.05.

(b) $[Ir_2(H)_4Cl(CO)_2(DPM)_2][BF_4]$ (4). An atmosphere of hydrogen was placed over a solution of $[Ir_2(CO)_2(\mu\text{-}Cl)(DPM)_2][BF_4]$ (**2**) (200 mg, 0.150 mmol) in 5 mL of CH_2Cl_2, and the mixture was stirred for 15 min resulting in a color change from dark red to light yellow. The solution was taken to dryness under a rapid flow of hydrogen leaving a pale yellow powder which proved to be susceptible to decomposition except when kept sealed under an atmosphere of hydrogen. For this reason no elemental analyses could be obtained.

(c) $[Ir_2(H)_2(CO)_2(\mu\text{-}Cl)(DPM)_2][BF_4]$ (5). Method A. An atmosphere of hydrogen was placed over a slurry of $[Ir_2(CO)_2(\mu\text{-}Cl)(DPM)_2][BF_4]$ (**2**) (200 mg, 0.150 mmol) in 10 mL of THF and the mixture stirred for 15 min, during which time all of the solid disappeared leaving a clear light yellow solution of **4**. The hydrogen atmosphere was replaced by one of dinitrogen, and the solution was refluxed for 20 min. During this time the color changed to a very intense yellow and a bright yellow flocculent precipitate appeared. The mixture was taken to dryness under an N_2 stream giving **5** as a bright yellow powder. Recrystallization from CH_2Cl_2/diethyl ether gave **5** as a bright yellow microcrystalline solid in 90% yield. A CH_2Cl_2 solution of this solid proved to be a 1:1 electrolyte ($\Lambda(10^{-3}$ M) = 54.2 $\Omega^{-1}\ cm^2\ mol^{-1}$). Anal. Calcd for $Ir_2ClP_4F_4O_2C_{52}BH_{46}$: C, 46.84; H, 3.48. Found: C, 46.76; H, 3.54.

Method B. To a slurry of **3** (200 mg, 0.156 mmol) in 10 mL of THF under dinitrogen was added dropwise 1 equiv of $AgBF_4$ (30.4 mg, 0.156 mmol) in 2 mL of THF. The color immediately changed to bright yellow, and upon continued stirring a yellow precipitate appeared. The solution was taken to dryness under a stream of dinitrogen. The product was extracted from the silver-containing products by adding 10 mL of CH_2Cl_2, filtering under dinitrogen to give a clear bright yellow solution. Product precipitation was induced by the addition of 30 mL of diethyl ether. The resulting bright yellow solid, obtained in 85% yield, was in all spectroscopic properties identical with the product obtained from method A.

(d) $[Ir_2(H)Cl_2(CH_3O_2CC{=}CHCO_2CH_3)(CO)_2(DPM)_2]\cdot CH_2Cl_2$ (6). To a solution of **3** (200 mg, 0.156 mmol) in 10 mL of CH_2Cl_2 under dinitrogen was added 1 equivalent to dimethyl acetylenedicarboxylate (DMA) (15.2 μL, 0.156 mmol) which produced an immediate color change from pale yellow to bright yellow. The solution was allowed to stir for 12 h, during which time a yellow solid precipitated from solution. Diethyl ether (30 mL) was added to ensure complete precipitation, and the resulting solid was collected and washed with two 10-mL portions of diethyl ether and finally dried under an N_2 stream giving **6** as a yellow microcrystalline solid in 90% yield. Compound **6** was determined to be nonconducting in CH_2Cl_2 solutions ($\Lambda(10^{-3}$ M) $\leq 0.5\ \Omega^{-1}\ cm^2\ mol^{-1}$). Anal. Calcd for $Ir_2Cl_4P_4O_6C_{59}H_{54}$: C, 46.96; H, 3.61. Found: C, 46.97; H, 3.69.

(e) $[Ir_2Cl_2(CH_3O_2CC{=}CHCO_2CH_3)_2(CO)_2(DPM)_2]$ (7). To a solution of **5** (200 mg, 0.150 mmol) in 10 mL of CH_2Cl_2 under dinitrogen was added an excess of DMA (50.0 μL, 0.513 mmol) which produced an immediate color change from yellow to orange. The solution was allowed to stir for 12 h, after which time 30 mL of diethyl ether was added resulting in the precipitation of a bright yellow flocculent solid. The solid was dissolved in acetone and placed on a chromatography column containing 100 mesh Florisil. Elution with acetone gave one bright yellow band which was collected as a yellow solution. The solution was taken to dryness under vacuum giving a bright yellow solid. Recrystallization from CH_2Cl_2/diethyl ether gave **7** as bright yellow crystals in 50% yield. Compound **7** was determined to be a nonelectrolyte in both CH_2Cl_2 and nitromethane solutions. Anal. Calcd for $Ir_2Cl_2P_4O_{10}C_{64}H_{58}$: C, 49.07; H, 3.73. Found: C, 48.78; H, 3.91.

X-ray Data Collection. Crystals of $[Ir_2Cl_2(CH_3O_2CC{=}CHCO_2CH_3)_2(CO)_2(DPM)_2]$ (**7**) of suitable quality for an X-ray study were obtained by the slow diffusion of diethyl ether into a saturated acetone solution of the complex. The crystals proved to be air stable so one was mounted on a glass fiber in the air and no special precautions were taken. Unit cell parameters were obtained from a least-squares refinement of the setting angles of 25 reflections, in the range $18.0° \leq 2\theta \leq 24.0°$, which were accurately centered on an Enraf-Nonius CAD4 diffractometer using Mo Kα radiation. The lack of systematic absences and the $\bar{1}$ diffraction symmetry were consistent with the space groups *P1* and *P*$\bar{1}$. The centrosymmetric space group was chosen and later verified by the successful refinement of the structure with acceptable positional parameters, thermal parameters, and agreement indices. A cell reduction failed to show the presence of a higher symmetry cell.[11]

(10) Typically a 1:1 electrolyte such as $[Rh_2(CO)_2(\mu\text{-}Cl)(\mu\text{-}CO)(DPM)_2][BF_4]$ gives a value of ca. 45 $\Omega^{-1}\ cm^2\ mol^{-1}$ in CH_2Cl_2.

(11) The cell reduction was performed by using a modification of TRACER II by S. L. Lawson. See: Lawson, S. L.; Jacobsen, R. A. "The Reduced Cell and Its Crystallographic Applications", Ames Laboratory Report IS-1141; USAEC: Iowa State University, Ames, IA, April 1965.

Table II. Summary of Crystal Data and Details of Intensity Collection

compd	$[Ir_2Cl_2(CH_3O_2CC{=}CHCO_2CH_3)_2(CO)_2(DPM)_2]$
fw	1566.35
formula	$Ir_2Cl_2P_4O_{10}C_{64}H_{58}$
cell parameters	
a, Å	15.978 (2)
b, Å	20.460 (5)
c, Å	21.494 (2)
α, deg	107.86 (2)
β, deg	90.46 (2)
γ, deg	106.17 (2)
V, Å^3	6389.8
d(calcd), g/cm^3	1.628
space group	$P\bar{1}$ (Z = 4)
temp, °C	22
radiatn (λ, Å)	graphite-monchromated Mo Kα (0.71069)
receiving aperture, mm	2.00 + 1.00 tan θ wide × 4.0 high, 173 from crystal
takeoff angle, deg	3.0
scan speed, deg/min	variable between 6.705 and 1.059
scan width	0.75 + 0.347 tan θ in ω
2θ limits, deg	$0.6 \le 2\theta \le 46.0$
no. of unique data collected	17756 ($+h, \pm k, \pm l$)
no. of unique data used	11275
range of transmissn factors	0.3291–0.4477
final no. of parameters refined	545
error in observn of unit weight	2.960
R	0.061
R_w	0.090

Intensity data were collected on a CAD4 diffractometer in the bisecting mode employing the ω–2θ scan technique up to 2θ = 46.0° with graphite-monochromated Mo Kα radiation. Backgrounds were scanned for 25% of the peak width on either end of the peak scan. The intensities of three standard reflections were measured every 1 h of exposure to assess possible crystal decomposition or movement. No significant variation in these standards were observed so no correction was applied to the data. A total of 17756 unique reflections were measured and processed in the usual way by using a value of 0.04 for p;[12] of these 11275 were considered to be observed and were used in subsequent calculations. Absorption corrections were applied to the data by using Gaussian integration.[13] See Table II for pertinent crystal data and details of data collection.

Structure Solution and Refinement. The structure was solved in the space group $P\bar{1}$ with two individual dimers per asymmetric unit. The positions of the four syntheses Ir atoms were obtained by using a combination of direct methods and Patterson techniques. Subsequent refinements and difference Fourier calculations led to the location of the other atoms. Atomic scattering factors were taken from Cromer and Waber's tabulation[14] for all atoms except hydrogen, for which the values of Stewart et al.[15] were used. Anomalous dispersion terms[16] for Ir, Cl, and P were included in F_c. The carbon atoms of all phenyl rings were refined as rigid groups having D_{6h} symmetry, C–C distances of 1.392 Å, and independent isotropic thermal parameters. All hydrogen atoms of the DPM ligands were located and included as fixed contributions in the least-squares refinements but were not themselves refined. Their idealized positions were calculated from the geometries about their attached carbon atoms using C–H distances of 0.95 Å. Hydrogen atoms were assigned isotropic thermal parameters of 1 Å^2 greater than the isotropic thermal parameter of their attached carbons. The olefinic hydrogens attached to carbons C(5A), C(5B), C(6A), and C(6B) were located and were included as fixed contributions as described above. No attempt was made to locate the methyl hydrogens of the methoxycarbonyl substituents. In the final refinements only the Ir, Cl, and P atoms were refined anisotropically owing to the large number of variables and the resulting high cost of the least-squares calculations.

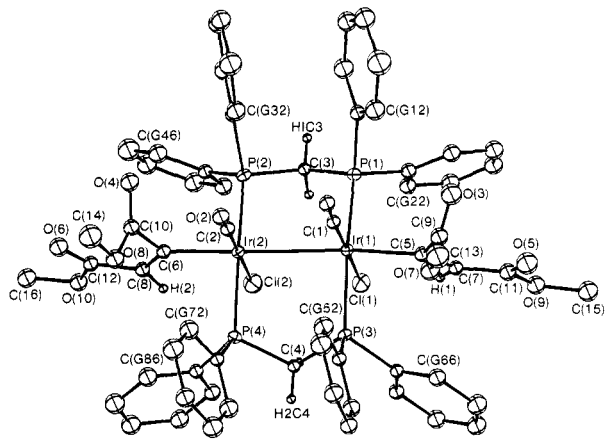

Figure 1. Perspective view of one of the two independent molecules (dimer A) of $[Ir_2Cl_2(CH_3O_2CC{=}CHCO_2CH_3)_2(CO)_2(DPM)_2]$ showing the numbering scheme. The numbering on the phenyl carbon atoms starts at the ones bonded to phosphorus and increases sequentially around the ring. The 20% thermal ellipsoids are shown for all atoms except hydrogen which are shown artifically small.

The final model with 545 parameters varied refined to R = 0.061 and R_w = 0.090.[17] On the final difference Fourier map, the 20 highest peaks (1.01–0.34 e Å^{-3}) were in the vicinities of the iridium and chlorine atoms. A typical carbon on earlier syntheses had a peak intensity of about 4.0 e Å^{-3}. The final positional parameters of the individual non-hydrogen atoms and the phenyl groups are given in Tables III and IV, respectively. The derived hydrogen positions, their thermal parameters, and a listing of observed and calculated structure amplitudes used in the refinements are available.[18]

Description of Structure

The title complex **7** crystallizes in the space group $P\bar{1}$ with two independent dimers per asymmetric unit. Although the dimers differ in their relative orientations, all the analogous bond lengths and angles (see Tables V and VI) associated with each are very similar confirming that there is no major difference between them. A perspective view of molecule A, including the numbering scheme, is shown in Figure 1. A view of the approximate equatorial plane of the metals is shown in Figure 2 along with some relevent average bond lengths and angles.

The overall geometry of the complex is essentially as expected for a binuclear species bridged by two mutually trans DPM ligands. Within the DPM framework, the bond lengths and angles are all normal (Tables V and VI) and similar to those found in other DPM-bridged complexes of iridium.[7-9,19,20] Each metal has a slightly distorted octahedral geometry in which the coordination sites are occupied by the two trans phosphorus atoms, a carbonyl group, a chloride ligand, a metalated olefin, and the Ir–Ir bond. The major distortion from octahedral geometry about each metal occurs in the P–Ir–P angles which are ca. 165.1° rather than 180° with all of the phosphorus atoms bent slightly toward the Cl ligands. This bending seems to arise in order to relieve some of the severe steric crowding in the complex. Each molecule possesses approximate C_{2v} geometry with a pseudomirror plane running

(12) Doedens, R. I.; Ibers, J. A. *Inorg. Chem.* **1967**, *6*, 204.
(13) For the programs used in the solution and refinement see ref 7.
(14) Cromer, D. T.; Waber, J. T. "International Tables for X-ray Crystallography"; Kynock Press: Birmingham, England, 1974; Vol. IV, Table 2.2 A.
(15) Stewart, R. F.; Davidson, E. R.; Simpson, W. T. *J. Chem. Phys.* **1965**, *42*, 3175.
(16) Cromer, D. T.; Liberman, D. *J. Chem. Phys.* **1970**, *53*, 1891.
(17) $R = \sum ||F_o| - |F_c||/\sum |F_o|$; $R_w = [\sum w(|F_o| - |F_c|)^2/\sum wF_o^2]^{1/2}$.
(18) Supplementary material.
(19) Kubiak, C. P.; Woodcock, C.; Eisenberg, R. *Inorg. Chem.* **1980**, *19*, 2733.
(20) Cowie, M.; Sutherland, B. R., unpublished results.

Table III. Positional and Isotropic Parameters for the Non-Group Atoms

atom	x^a	y	z	B, Å^2	atom	x	y	z	B, Å^2
Ir(1A)	0.42371 (5)	0.24036 (4)	−0.15032 (3)	2.75[b]	C(1A)	0.4577 (12)	0.3378 (10)	−0.1273 (9)	3.4 (4)
Ir(1B)	−0.24685 (5)	0.24364 (4)	0.35311 (3)	2.73[b]	C(1B)	−0.2060 (12)	0.3403 (10)	0.3818 (9)	3.5 (4)
Ir(2A)	0.25200 (4)	0.24104 (4)	−0.20866 (3)	2.82[b]	C(2A)	0.2867 (12)	0.3375 (11)	−0.1787 (9)	4.0 (4)
Ir(2B)	−0.07859 (5)	0.24376 (4)	0.28990 (3)	2.70[b]	C(2B)	−0.0478 (12)	0.3414 (10)	0.3169 (9)	3.6 (4)
Cl(1A)	0.3756 (4)	0.1129 (4)	−0.1863 (3)	7.1[b]	C(3A)	0.3869 (11)	0.1783 (9)	−0.3169 (8)	3.0 (3)
Cl(1B)	−0.2940 (4)	0.1163 (4)	0.3123 (3)	7.1[b]	C(3B)	−0.2664 (11)	0.1848 (9)	0.1865 (8)	3.2 (4)
Cl(2A)	0.2060 (4)	0.1141 (4)	−0.2462 (3)	7.6[b]	C(4A)	0.2406 (11)	0.1791 (9)	−0.0781 (8)	3.1 (3)
Cl(2B)	−0.1243 (5)	0.1168 (4)	0.2554 (3)	7.8[b]	C(4B)	−0.1035 (11)	0.1842 (9)	0.4225 (9)	3.5 (4)
P(1A)	0.4776 (3)	0.2210 (3)	−0.2533 (2)	3.3[b]	C(5A)	0.5384 (13)	0.2380 (10)	−0.1041 (9)	4.0 (4)
P(1B)	−0.3161 (3)	0.2327 (2)	0.2535 (2)	2.4[b]	C(5B)	−0.3651 (11)	0.2410 (9)	0.3930 (8)	3.1 (4)
P(2A)	0.3049 (3)	0.2242 (2)	−0.3126 (2)	3.2[b]	C(6A)	0.1339 (12)	0.2383 (10)	−0.2533 (9)	3.5 (4)
P(2B)	−0.1487 (3)	0.2255 (2)	0.1871 (2)	3.0[b]	C(6B)	0.0406 (11)	0.2410 (9)	0.2492 (8)	2.8 (3)
P(3A)	0.3587 (3)	0.2256 (2)	−0.0558 (2)	3.0[b]	C(7A)	0.5591 (12)	0.1765 (10)	−0.1097 (9)	3.7 (4)
P(3B)	−0.1894 (3)	0.2265 (2)	0.4462 (2)	3.0[b]	C(7B)	−0.4252 (12)	0.1822 (19)	0.3938 (9)	3.8 (4)
P(4A)	0.1841 (3)	0.2241 (3)	−0.1161 (2)	3.2[b]	C(8A)	0.0670 (13)	0.1798 (10)	−0.2816 (9)	3.9 (4)
P(4B)	−0.0182 (3)	0.2297 (2)	0.3825 (2)	2.7[b]	C(8B)	0.0573 (13)	0.1824 (10)	0.2104 (9)	4.0 (4)
O(1A)	0.4829 (9)	0.3987 (7)	−0.1133 (6)	4.7 (3)	C(9A)	0.6040 (15)	0.3089 (12)	−0.0683 (12)	5.6 (5)
O(1B)	−0.1806 (9)	0.4013 (7)	0.4037 (7)	5.0 (3)	C(9B)	−0.3769 (13)	0.3129 (11)	0.4250 (10)	4.2 (4)
O(2A)	0.3072 (9)	0.3977 (8)	−0.1577 (7)	5.5 (3)	C(10A)	0.1252 (14)	0.3081 (11)	−0.2546 (10)	4.7 (5)
O(2B)	−0.0274 (9)	0.4038 (7)	0.3325 (6)	4.9 (3)	C(10B)	0.1059 (13)	0.3121 (10)	0.2659 (10)	4.0 (4)
O(3A)	0.6620 (12)	0.3383 (10)	−0.0951 (9)	8.0 (5)	C(11A)	0.6378 (15)	0.1764 (12)	−0.0752 (11)	5.3 (5)
O(3B)	−0.3622 (10)	0.3470 (8)	0.4830 (8)	6.1 (4)	C(11B)	−0.5099 (13)	0.1848 (11)	0.4212 (10)	4.3 (4)
O(4A)	0.1647 (10)	0.3377 (8)	−0.2919 (8)	6.2 (4)	C(12A)	−0.0116 (13)	0.1775 (11)	−0.3193 (10)	4.1 (4)
O(4B)	0.1525 (10)	0.3379 (8)	0.3184 (7)	5.7 (3)	C(12B)	0.1409 (13)	0.1816 (11)	0.1831 (10)	4.3 (4)
O(5A)	0.6936 (12)	0.2289 (10)	−0.0395 (9)	8.2 (5)	C(13A)	0.6294 (21)	0.4156 (17)	0.0243 (16)	10.1 (9)
O(5B)	−0.5425 (11)	0.2338 (9)	0.4368 (8)	7.1 (4)	C(13B)	−0.3929 (24)	0.4213 (20)	0.4124 (18)	12.5 (11)
O(6A)	−0.0308 (10)	0.2311 (8)	−0.3220 (8)	6.2 (4)	C(14A)	0.0960 (20)	0.4155 (17)	−0.1968 (15)	9.7 (9)
O(6B)	0.2090 (11)	0.2309 (9)	0.1944 (8)	7.2 (4)	C(14B)	0.1718 (17)	0.4191 (14)	0.2445 (13)	7.3 (7)
O(7A)	0.5783 (11)	0.3383 (9)	−0.0128 (8)	6.8 (4)	C(15A)	0.7244 (17)	0.1049 (14)	−0.0541 (13)	7.3 (6)
O(7B)	−0.3970 (10)	0.3391 (8)	0.3807 (7)	6.0 (4)	C(15B)	−0.6477 (17)	0.1103 (13)	0.4487 (12)	6.9 (6)
O(8A)	0.0908 (10)	0.3392 (8)	−0.2037 (8)	6.1 (4)	C(16A)	−0.1479 (16)	0.1093 (13)	−0.3836 (12)	6.3 (6)
O(8B)	0.1091 (9)	0.3460 (7)	0.2223 (7)	4.9 (3)	C(16B)	0.2198 (16)	0.1089 (13)	0.1149 (12)	6.5 (6)
O(9A)	0.6487 (10)	0.1113 (8)	−0.0863 (7)	5.9 (4)	H(1A)	0.5118	0.1329	−0.1356	4.6
O(9B)	−0.5572 (10)	0.1177 (8)	0.4224 (7)	6.1 (4)	H(1B)	−0.4111	0.1373	0.3801	4.8
O(10A)	−0.0674 (9)	0.1137 (8)	−0.3459 (7)	5.6 (3)	H(2A)	0.0700	0.1356	−0.2764	4.5
O(10B)	0.1398 (9)	0.1153 (7)	0.1443 (7)	5.3 (3)	H(2B)	0.0123	0.1373	0.1992	5.0

[a] Estimated standard deviations in the last significant figures are given in parentheses in this and all subsequent tables. [b] Equivalent isotropic B's for anisotropic atoms.

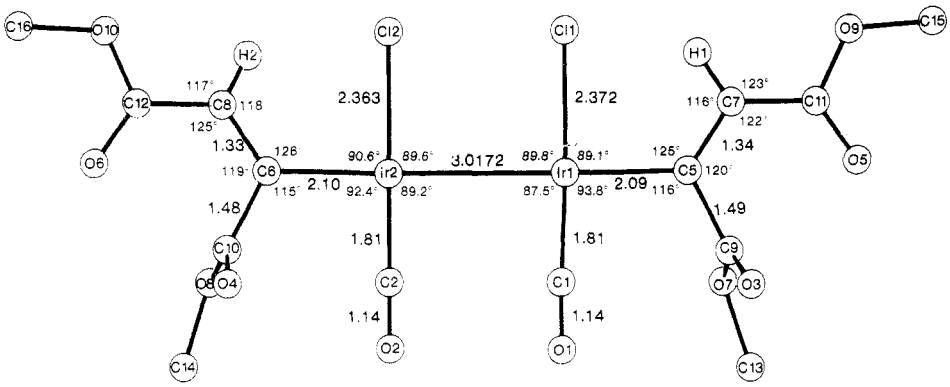

Figure 2. Representation of the complex in the approximate plane of the metals and the metalated olefin groups. Some relevant parameters, averaged over the two independent dimers, are shown.

perpendicular to the Ir–Ir bond (see Figure 2).

The iridium–iridium distances of 3.0128 (10) and 3.0216 (10) Å are extremely long and fall outside the range normally associated with Ir–Ir single bonds in analogous Ir–DPM systems (range 2.779 (1)–2.893 (2) Å).[7,9,19,20] However, electron-counting rules require a formal metal–metal bond, otherwise each metal would have a 17-electron configuration and consequently be paramagnetic, for which there is no evidence. The long metal–metal separation is possibly a result of the steric crowding about the Ir atoms. Bringing the metals closer together would result in highly unfavorable interactions between the two chlorine atoms and the two carbonyl groups. These distances are already rather short, at ca. 2.99 and 2.92 Å, respectively. In a somewhat analogous complex, $[Ir_2Cl_4(CO)_2(DPM)_2]$, which also has pseudooctahedral Ir centers and cis Cl ligands, the metal–metal distance has a more typical value of 2.786 (1) Å.[20] However, in this case the molecule is twisted about the Ir–Ir bond by ca. 27.7° such that the ligands on one metal are staggered with respect to those on the other metal, reducing the unfavorable contacts and allowing a normal metal–metal interaction. In the present complex both halves of the molecule are almost exactly eclipsed. It seems that staggering about the two metals is not possible owing to the unfavorable contacts that would result between the metalated olefins and the DPM phenyl groups. In another crowded binuclear complex containing pseudooctahedral metal centers, $[Rh_2(CN\text{-}t\text{-}Bu)_4(\mu\text{-}CF_3C_2CF_3)(DPM)_2][PF_6]_2$,[21] the molecule was found to be

(21) Mague, J. T. *Inorg. Chem.* **1983**, *22*, 1158.

Table IV. Derived Parameters for the Rigid-Group Atoms of $[Ir_2Cl_2(CH_3O_2CC{=}CHCO_2CH_3)_2(CO)_2(DPM)_2]$

atom	x	y	z	B, Å²	atom	x	y	z	B, Å²
C(G11A)	0.5511 (9)	0.2948 (7)	−0.2780 (8)	4.1 (4)	C(G31A)	0.3566 (9)	0.3013 (7)	−0.3426 (7)	4.2 (4)
C(G12A)	0.6037 (11)	0.3562 (9)	−0.2306	7.4 (6)	C(G32A)	0.3899 (11)	0.3703 (9)	−0.2981 (5)	6.5 (6)
C(G13A)	0.6605 (11)	0.4103 (8)	−0.2495 (8)	10.5 (5)	C(G33A)	0.4327 (11)	0.4270 (6)	−0.3202 (8)	9.1 (8)
C(G14A)	0.6647 (10)	0.4031 (8)	−0.3158 (10)	7.7 (7)	C(G34A)	0.4422 (10)	0.4145 (8)	−0.3868 (9)	7.1 (6)
C(G15A)	0.6121 (11)	0.3417 (10)	−0.3632 (6)	6.5 (6)	C(G35A)	0.4090 (11)	0.3455 (9)	−0.4312 (6)	6.3 (6)
C(G16A)	0.553 (10)	0.2876 (7)	−0.3443 (7)	6.9 (6)	C(G36A)	0.3661 (10)	0.2889 (6)	−0.4091 (7)	6.7 (6)
C(G11B)	−0.3244 (10)	0.3100 (6)	0.2343 (7)	3.2 (4)	C(G31B)	−0.1366 (9)	0.3010 (6)	0.1551 (6)	3.2 (4)
C(G12B)	−0.2607 (8)	0.3758 (8)	0.2616 (7)	5.5 (5)	C(G32B)	−0.0646 (8)	0.3620 (7)	0.1772 (6)	5.5 (5)
C(G13B)	−0.2672 (10)	0.4360 (6)	0.2469 (8)	6.9 (6)	C(G33B)	−0.0536 (8)	0.4168 (6)	0.1496 (7)	5.7 (5)
C(G14B)	−0.3375 (13)	0.4304 (8)	0.2049 (1)	7.4 (6)	C(G34B)	−0.1148 (11)	0.4106 (7)	0.1001 (7)	6.1 (5)
C(G15B)	−0.4013 (10)	0.3646 (11)	0.1777 (8)	11.6 (11)	C(G35B)	−0.1868 (9)	0.3496 (9)	0.0780 (6)	7.3 (6)
C(G16B)	−0.3947 (9)	0.3044 (8)	0.1924 (8)	8.6 (8)	C(G36B)	−0.1978 (7)	0.2948 (6)	0.1056 (7)	5.6 (5)
C(G21A)	0.5416 (9)	0.1567 (7)	−0.2698 (7)	4.3 (4)	C(G41A)	0.2232 (8)	0.1615 (7)	−0.3803 (6)	3.8 (4)
C(G22A)	0.5029 (7)	0.0834 (7)	−0.3003 (7)	5.0 (5)	C(G42A)	0.2144 (9)	0.0882 (8)	−0.4008 (7)	5.6 (5)
C(G23A)	0.5537 (10)	0.0364 (5)	−0.3113 (7)	6.4 (6)	C(G43A)	0.1534 (11)	0.0415 (6)	−0.4533 (8)	6.9 (6)
C(G24A)	0.6433 (9)	0.0627 (8)	−0.2918 (8)	6.4 (6)	C(G44A)	0.1011 (9)	0.0680 (9)	−0.4852 (7)	7.1 (6)
C(G25A)	0.6820 (7)	0.1360 (8)	−0.2613 (8)	6.2 (6)	C(G45A)	0.1099 (10)	0.1413 (9)	−0.4648 (8)	8.3 (8)
C(G26A)	0.6312 (9)	0.1830 (6)	−0.2503 (7)	5.6 (5)	C(G46A)	0.1709 (10)	0.1880 (6)	−0.4123 (8)	6.2 (6)
C(G21B)	−0.4272 (7)	0.1714 (6)	0.2360 (7)	3.9 (4)	C(G41B)	−0.1197 (8)	0.1620 (6)	0.1181 (5)	3.4 (4)
C(G22B)	−0.4448 (8)	0.0984 (7)	0.2022 (7)	4.4 (4)	C(G42B)	−0.1537 (8)	0.0886 (7)	0.1076 (6)	4.4 (4)
C(G23B)	−0.5305 (10)	0.0534 (5)	0.1910 (7)	6.5 (6)	C(G43B)	−0.1287 (9)	0.0397 (5)	0.0560 (7)	5.7 (5)
C(G24B)	−0.5986 (7)	0.0814 (8)	0.2136 (8)	6.8 (6)	C(G44B)	−0.0697 (10)	0.0641 (7)	0.0150 (6)	5.8 (5)
C(G25B)	−0.5811 (8)	0.1544 (8)	0.2475 (8)	6.9 (6)	C(G45B)	−0.0357 (9)	0.1376 (8)	0.0255 (6)	6.0 (6)
C(G26B)	−0.4954 (10)	0.1994 (6)	0.2586 (7)	5.2 (5)	C(G46B)	−0.0607 (8)	0.1865 (5)	0.0771 (7)	4.4 (4)
C(G51A)	0.3621 (9)	0.2994 (7)	0.0194 (5)	3.8 (4)	C(G71A)	0.1691 (9)	0.2982 (7)	−0.0489 (6)	3.4 (4)
C(G52A)	0.3859 (10)	0.3699 (8)	0.0185 (6)	6.9 (6)	C(G72A)	0.1695 (10)	0.3626 (8)	−0.0583 (6)	6.7 (6)
C(G53A)	0.3915 (11)	0.4262 (6)	0.0762 (1)	8.5 (7)	C(G73A)	0.1526 (11)	0.4170 (6)	−0.0074 (9)	8.1 (7)
C(G54A)	0.3734 (11)	0.4121 (7)	0.1348 (7)	6.9 (6)	C(G14A)	0.1351 (10)	0.4070 (8)	0.0529 (7)	6.6 (6)
C(G55A)	0.3496 (10)	0.3416 (9)	0.1357 (5)	5.7 (5)	C(G75A)	0.1347 (11)	0.3426 (9)	0.0623 (6)	7.8 (7)
C(G56A)	0.3439 (9)	0.2853 (6)	0.0781 (7)	5.6 (5)	C(G76A)	0.1517 (10)	0.2881 (7)	0.0114 (8)	6.6 (6)
C(G51B)	−0.1456 (8)	0.3015 (6)	0.5213 (5)	3.5 (4)	C(G71B)	0.0484 (8)	0.3058 (6)	0.4491 (6)	3.6 (4)
C(G52B)	−0.1680 (8)	0.3650 (7)	0.5332 (6)	4.4 (4)	C(G72B)	0.0369 (9)	0.3732 (8)	0.4595 (7)	5.5 (5)
C(G53B)	−0.1339 (10)	0.4218 (6)	0.5909 (7)	5.9 (5)	C(G73B)	0.0851 (10)	0.4317 (6)	0.5118 (8)	6.3 (6)
C(G54B)	−0.0774 (10)	0.4151 (7)	0.6366 (6)	6.4 (6)	C(G74B)	0.1448 (10)	0.4228 (7)	0.5537 (6)	6.3 (6)
C(G55B)	−0.0550 (9)	0.3516 (8)	0.6247 (6)	7.0 (6)	C(G75B)	0.1563 (9)	0.3555 (9)	0.5433 (7)	9.0 (8)
C(G56B)	−0.0891 (9)	0.2948 (6)	0.5670 (7)	5.4 (5)	C(G76B)	0.1081 (10)	0.2969 (7)	0.4910 (8)	5.9 (5)
C(G61A)	0.3929 (8)	0.1630 (6)	−0.0246 (6)	3.2 (3)	C(G81A)	0.0767 (7)	0.1624 (7)	−0.1373 (7)	3.7 (4)
C(G62A)	0.3505 (7)	0.0895 (7)	−0.0477 (6)	5.4 (5)	C(G82A)	0.0599 (8)	0.0886 (7)	−0.1512 (7)	4.8 (5)
C(G63A)	0.3777 (9)	0.0430 (5)	−0.0224 (7)	5.5 (5)	C(G83A)	−0.0259 (10)	0.0437 (5)	−0.1666 (7)	6.0 (5)
C(G64A)	0.4474 (10)	0.0699 (8)	0.0266 (7)	6.0 (5)	C(G84A)	−0.0948 (7)	0.0725 (8)	−0.1681 (8)	6.7 (6)
C(G65A)	0.4899 (8)	0.1434 (8)	0.0502 (6)	8.0 (7)	C(G85A)	−0.0780 (8)	0.1463 (9)	−0.1542 (8)	7.2 (6)
C(G66A)	0.4626 (8)	0.1900 (5)	0.0249 (7)	5.3 (5)	C(G86A)	0.0077 (10)	0.1912 (6)	−0.1388 (8)	6.3 (6)
C(G61B)	−0.2643 (8)	0.1630 (6)	0.4778 (6)	3.4 (4)	C(G81B)	0.0491 (8)	0.1680 (6)	0.3637 (7)	3.6 (4)
C(G62B)	−0.2836 (9)	0.0893 (7)	0.4464 (5)	4.4 (4)	C(G82B)	0.0118 (7)	0.0953 (7)	0.3550 (7)	4.5 (4)
C(G63B)	−0.3427 (9)	0.0415 (5)	0.4709 (7)	5.7 (5)	C(G83B)	0.0632 (10)	0.0488 (5)	0.3399 (7)	6.0 (5)
C(G64B)	−0.3825 (9)	0.0673 (7)	0.5268 (7)	6.3 (6)	C(G84B)	0.1519 (9)	0.0749 (8)	0.3335 (8)	7.0 (6)
C(G65B)	−0.3633 (10)	0.1410 (8)	0.5581 (6)	6.5 (6)	C(G85B)	0.1891 (7)	0.1476 (8)	0.3422 (8)	6.3 (6)
C(G66B)	−0.3042 (9)	0.1888 (5)	0.5336 (6)	5.1 (5)	C(G86B)	0.1377 (9)	0.1942 (6)	0.3573 (7)	6.1 (5)

Rigid-Group Parameters

	x_c[a]	y_c	z_c	δ	ϵ	η
ring 1A	0.6079 (7)	0.3490 (6)	−0.2969 (6)	2.11 (3)	1.94 (1)	−1.28 (3)
ring 2A	−0.3310 (7)	0.3702 (6)	0.2196 (5)	1.768 (11)	2.618 (10)	−0.243 (11)
ring 3A	0.5924 (6)	0.1097 (5)	−0.2808 (4)	−1.044 (9)	−2.794 (9)	−0.235 (9)
ring 4A	−0.5129 (6)	0.1264 (5)	0.2248 (4)	0.382 (10)	−2.604 (9)	−3.062 (10)
ring 5A	0.3994 (6)	0.3579 (6)	−0.3647 (5)	2.73 (3)	1.956 (9)	−1.68 (3)
ring 6A	−0.1257 (6)	0.3558 (5)	0.1276 (4)	1.722 (10)	2.593 (9)	−0.511 (10)
ring 7A	0.1622 (6)	0.1148 (6)	−0.4328 (5)	0.280 (9)	3.072 (9)	−2.361 (9)
ring 8A	−0.0947 (6)	0.1131 (5)	0.0665 (4)	−0.671 (9)	2.817 (8)	−0.977 (9)
ring 1B	0.3677 (6)	0.3558 (5)	0.0771 (5)	2.822 (12)	−2.580 (9)	1.461 (11)
ring 2B	−0.1115 (6)	0.3583 (5)	0.5790 (4)	−2.602 (9)	−2.904 (8)	2.157 (9)
ring 3B	0.4202 (6)	0.1165 (5)	0.0013 (4)	−1.010 (10)	−2.567 (8)	0.419 (10)
ring 4B	−0.3234 (6)	0.1151 (5)	0.5023 (4)	0.200 (12)	−2.288 (8)	2.435 (13)
ring 5B	0.1521 (6)	0.3526 (6)	0.0020 (5)	3.000 (13)	−2.494 (9)	1.296 (12)
ring 6B	0.0966 (6)	0.3643 (5)	0.5014 (5)	−2.661 (10)	−2.919 (9)	2.320 (9)
ring 7B	−0.0091 (6)	0.1175 (5)	−0.1527 (4)	0.340 (9)	−3.001 (9)	−3.010 (9)
ring 8B	0.1005 (6)	0.1215 (5)	0.3486 (4)	−0.925 (8)	3.079 (9)	−0.284 (9)

[a] x_c, y_c, and z_c are the fractional coordinates of the centroid of the rigid group. [b] The rigid group orientation angles δ, ϵ, and η (radians) are the angles by which the rigid body is rotated with respect to a set of axes x, y, and z. See: La Placa, S. J.; Ibers, J. A. *Acta Crystallogr.* **1965**, *18*, 511.

twisted about the Rh–Rh axis by ca. 20.3° and the Rh–Rh distance is still very long (2.9653 (6) Å) although the complex again has a metal–metal bond. It is also possible that the long Ir–Ir bond in **7** is a result of the high trans influence of the two metalloolefin groups which lie opposite the Ir–Ir bond.

The Ir–Cl distances and the parameters involving the carbonyl ligands are all normal and compare well with

Table V. Selected Distances (Å) in $[Ir_2Cl_2(CH_3O_2CC{=}CHCO_2CH_3)_2(CO)_2(DPM)_2]$

Bonding Distances

	dimer A	dimer B		dimer A	dimer B
Ir(1)–Ir(2)	3.0128 (10)	3.0216 (10)	C(12)–O(6)	1.24 (2)	1.22 (2)
Ir(1)–Cl(1)	2.372 (8)	2.371 (7)	C(9)–O(7)	1.29 (2)	1.30 (2)
Ir(2)–Cl(2)	2.362 (8)	2.364 (8)	C(10)–O(8)	1.30 (2)	1.32 (2)
Ir(1)–P(1)	2.342 (5)	2.320 (5)	C(11)–O(9)	1.34 (2)	1.38 (2)
Ir(1)–P(3)	2.353 (5)	2.355 (5)	C(12)–O(10)	1.31 (2)	1.35 (2)
Ir(2)–P(2)	2.354 (5)	2.346 (5)	C(13)–O(7)	1.52 (3)	1.59 (4)
Ir(2)–P(4)	2.345 (5)	2.335 (5)	C(14)–O(8)	1.50 (3)	1.48 (3)
Ir(1)–C(1)	1.82 (2)	1.80 (2)	C(15)–O(9)	1.45 (3)	1.54 (3)
Ir(2)–C(2)	1.80 (2)	1.82 (2)	C(16)–O(10)	1.48 (3)	1.45 (3)
Ir(1)–C(5)	2.10 (2)	2.08 (2)	P(1)–C(3)	1.81 (2)	1.80 (2)
Ir(2)–C(6)	2.09 (2)	2.11 (2)	P(2)–C(3)	1.80 (2)	1.83 (2)
C(1)–O(1)	1.14 (2)	1.14 (2)	P(3)–C(4)	1.84 (2)	1.81 (2)
C(2)–O(2)	1.12 (2)	1.16 (2)	P(4)–C(4)	1.80 (2)	1.81 (2)
C(5)–C(7)	1.36 (2)	1.32 (2)	P(1)–C(G11)	1.86 (2)	1.79 (2)
C(6)–C(8)	1.33 (2)	1.33 (2)	P(1)–C(G21)	1.84 (2)	1.82 (1)
C(5)–C(9)	1.50 (3)	1.48 (2)	P(2)–C(G31)	1.87 (2)	1.84 (2)
C(6)–C(10)	1.48 (3)	1.47 (2)	P(2)–C(G41)	1.83 (1)	1.81 (1)
C(7)–C(11)	1.45 (3)	1.49 (3)	P(3)–C(G51)	1.83 (1)	1.82 (1)
C(8)–C(12)	1.47 (3)	1.46 (3)	P(3)–C(G61)	1.82 (2)	1.81 (1)
C(9)–O(3)	1.21 (2)	1.21 (2)	P(4)–C(G71)	1.82 (1)	1.81 (1)
C(10)–O(4)	1.22 (2)	1.23 (2)	P(4)–C(G81)	1.78 (1)	1.83 (2)
C(11)–O(5)	1.22 (2)	1.21 (2)			

Nonbonding Distances

	dimer A	dimer B		dimer A	dimer B
P(1)–P(2)	3.057 (7)	3.061 (6)	Cl(1)–Cl(2)	3.000 (9)	2.982 (9)
P(3)–P(4)	3.056 (7)	3.061 (7)	C(1)–C(2)	2.94 (3)	2.89 (2)
H(1)–Cl(1)	2.30	2.43	O(1)–O(2)	2.95 (2)	2.89 (2)
H(2)–Cl(2)	2.45	2.50			

values previously reported.[7-9,19,20]

As can be seen in Figures 1 and 2, the alkyne molecules have inserted into the two original Ir–H bonds forming two metalloolefin linkages, in which the CO_2CH_3 groups are mutually cis about the C=C bonds. The C=C distances (average 1.34 Å) are typical of carbon–carbon double bonds and the angles about these carbon atoms are all close to 120° (see Table VI), consistent with sp^2 hybridization. The Ir–C(olefin) distances (average 2.10 Å) are normal and compare well with similar values involving σ-bonded carbon atoms.[22,23] Within each of the metalated olefin groups, one CO_2CH_3 group lies in the metal–olefin plane while the other is essentially perpendicular to it, again likely a result of intramolecular nonbonded contacts. As a result, the C=O fragment of one of the CO_2CH_3 groups is coplanar with the olefin linkage and could in principle be conjugated with it. However, as the bond lengths indicate, there is no significant difference between the two CO_2CH_3 groups of each metalated olefin. All of the bond lengths and angles associated with the olefin atoms are unexceptional and similar to those observed in other structures.[5,6] One feature of note concerning the metalloolefin groups is that the severe crowding around the metals leads to rather short olefinic hydrogen–chlorine contacts of ca. 2.42 Å.

Discussion and Results

Placing an atmosphere of H_2 over a solution of *trans*-$[IrCl(CO)(DPM)]_2$, **1**, produces an immediate reaction as evidenced by a rapid color change from purple to yellow. The new compound **3** which is isolated from this solution displays two distinct terminal carbonyl bands (2012, 1972 cm^{-1}) and two terminal hydride bands (2222, 2091 cm^{-1}) in the infrared spectrum while analyses indicate the presence of two chlorines per dimer. On the basis of this information, **3** is formulated to have the structure shown below in the solid state. This geometry is analogous to

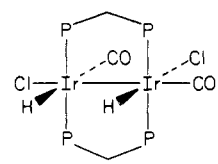

3

that postulated for the products of the reaction of **1** with alkynes, and confirmed by an X-ray structure of the DMA adduct.[8] The spectroscopic parameters for **3** and these alkyne adducts are very similar. Evidence that the two hydride ligands are not on the same metal comes from selective phosphorus decoupled ^1H NMR experiments (vide infra). The conversion of **1** to **3** can readily be reversed by gently warming the solution under N_2 for several minutes, suggesting that the two hydride ligands are mutually cis.

With mononuclear octahedral bis(phosphine)iridium hydrides as a basis for comparison, the carbonyl and iridium–hydride stretches of **3** can be assigned. In mononuclear systems, Ir–H stretches, when H is trans to CO, are generally observed in the range 2100–2000 cm^{-1}, while those when the hydride ligand is trans to ligands such as halides occur around 2240–2180 cm^{-1}.[24] A similar trend is observed for the carbonyl bands; where CO is trans to a hydride ligand, ν(CO) occurs at ca. 1980 cm^{-1}, while the carbonyl stretch when CO is trans to a chloride ligand is observed at ca. 2025 cm^{-1}.[24] With this information, we assign the carbonyl stretch at 1972 cm^{-1} as due to the group opposite the hydride ligand and that at 2012 cm^{-1} as the CO opposite the Ir–Ir bond. Similarly, the Ir–H stretch at 2222 cm^{-1} would appear to arise from the hydride ligand opposite the chloro ligand and that at 2091 cm^{-1} due to the hydride opposite the carbonyl group. The observed

(22) Diversi, P.; Ingrosso, G.; Lucherini, A.; Porzio, W.; Zocchi, M. *Inorg. Chem.* **1980**, *19*, 3590.
(23) Crabtree, R. H.; Quirk, J. M.; Felkin, H.; Fillebeen-Khan, T.; Pascard, C. *J. Organomet. Chem.* **1980**, *187*, C32.
(24) Kaesz, H. D.; Saillant, R. B. *Chem. Rev.* **1972**, *72*, 231.

Table VI. Selected Angles (deg) in $[Ir_2Cl_2(CH_3O_2CC{=}CHCO_2CH_3)_2(CO)_2(DPM)_2]$

	dimer A	dimer B		dimer A	dimer B
P(1)-Ir(1)-Ir(2)	90.7 (1)	89.7 (1)	O(3)-C(9)-O(7)	126 (2)	123 (2)
P(3)-Ir(1)-Ir(2)	90.2 (1)	91.4 (1)	O(4)-C(10)-O(8)	125 (2)	123 (2)
P(2)-Ir(2)-Ir(1)	90.4 (1)	91.2 (1)	O(5)-C(11)-O(9)	119 (2)	120 (2)
P(4)-Ir(2)-Ir(1)	90.9 (1)	89.6 (1)	O(6)-C(12)-O(10)	119 (2)	119 (2)
P(1)-Ir(1)-P(3)	163.4 (2)	167.1 (1)	C(9)-O(7)-C(13)	117 (2)	111 (2)
P(2)-Ir(2)-P(4)	164.5 (2)	165.2 (2)	C(10)-O(8)-C(14)	114 (2)	113 (2)
Cl(1)-Ir(1)-Ir(2)	89.8 (2)	89.7 (2)	C(11)-O(9)-C(15)	119 (2)	117 (2)
Cl(2)-Ir(2)-Ir(1)	89.9 (2)	89.3 (2)	C(12)-O(10)-C(16)	117 (2)	117 (2)
P(1)-Ir(1)-Cl(1)	82.2 (2)	83.2 (2)	P(1)-C(3)-P(2)	115.9 (9)	114.7 (9)
P(3)-Ir(1)-Cl(1)	82.2 (2)	84.0 (2)	P(3)-C(4)-P(4)	113.9 (9)	115 (1)
P(2)-Ir(2)-Cl(2)	82.3 (2)	83.0 (2)	Ir(1)-P(1)-C(3)	109.3 (6)	110.0 (6)
P(4)-Ir(2)-Cl(2)	82.3 (2)	82.2 (2)	Ir(1)-P(1)-C(G11)	122.5 (4)	121.3 (4)
P(1)-Ir(1)-C(1)	95.6 (6)	96.6 (6)	Ir(1)-P(1)-C(G21)	113.3 (5)	113.3 (5)
P(3)-Ir(1)-C(1)	99.9 (6)	96.3 (6)	Ir(2)-P(2)-C(3)	108.7 (6)	108.9 (6)
P(2)-Ir(2)-C(2)	98.7 (6)	96.3 (6)	Ir(2)-P(2)-C(G31)	122.0 (4)	120.6 (3)
P(4)-Ir(2)-C(2)	96.7 (6)	98.5 (6)	Ir(2)-P(2)-C(G41)	113.5 (4)	115.6 (4)
P(1)-Ir(1)-C(5)	93.2 (5)	88.4 (5)	Ir(1)-P(3)-C(4)	109.0 (6)	108.6 (6)
P(3)-Ir(1)-C(5)	85.7 (5)	90.3 (5)	Ir(1)-P(3)-C(G51)	124.5 (4)	121.2 (4)
P(2)-Ir(2)-C(6)	87.3 (5)	91.3 (5)	Ir(1)-P(3)-C(G61)	113.9 (4)	115.2 (4)
P(4)-Ir(2)-C(6)	91.0 (5)	87.5 (5)	Ir(2)-P(4)-C(4)	109.6 (6)	110.3 (6)
Cl(1)-Ir(1)-C(1)	176.7 (6)	177.0 (6)	Ir(2)-P(4)-C(G71)	122.5 (5)	121.9 (5)
Cl(2)-Ir(2)-C(2)	179.0 (6)	177.8 (6)	Ir(2)-P(4)-C(G81)	112.4 (5)	114.0 (4)
Cl(1)-Ir(1)-C(5)	89.2 (5)	89.0 (5)	C(G11)-P(1)-C(G21)	100.9 (7)	104.9 (6)
Cl(2)-Ir(2)-C(6)	85.5 (5)	89.2 (5)	C(G11)-P(1)-C(3)	105.6 (8)	105.6 (8)
C(1)-Ir(1)-C(5)	93.5 (8)	94.1 (7)	C(G21)-P(1)-C(3)	103.5 (7)	99.3 (6)
C(2)-Ir(2)-C(6)	91.9 (8)	92.9 (7)	C(G31)-P(2)-C(G41)	104.2 (6)	100.3 (6)
C(1)-Ir(1)-Ir(2)	87.7 (6)	87.3 (6)	C(G31)-P(2)-C(3)	104.3 (2)	106.7 (8)
C(2)-Ir(2)-Ir(1)	89.8 (7)	88.6 (6)	C(G41)-P(2)-C(3)	102.0 (6)	103.1 (6)
C(5)-Ir(1)-Ir(2)	175.8 (5)	177.8 (5)	C(G51)-P(3)-C(G61)	102.1 (6)	101.1 (5)
C(6)-Ir(2)-Ir(1)	177.3 (5)	176.9 (5)	C(G51)-P(3)-C(4)	103.5 (7)	106.8 (6)
Ir(1)-C(1)-O(1)	177 (2)	176 (2)	C(G61)-P(3)-C(4)	101.0 (7)	102.1 (7)
Ir(2)-C(2)-O(2)	177 (2)	178 (2)	C(G71)-P(4)-C(G81)	103.0 (6)	103.1 (6)
Ir(1)-C(5)-C(7)	124 (1)	125 (1)	C(G71)-P(4)-C(4)	105.1 (7)	104.0 (6)
Ir(2)-C(6)-C(8)	126 (1)	125 (1)	C(G81)-P(4)-C(4)	102.2 (7)	101.1 (8)
Ir(1)-C(5)-C(9)	117 (1)	114 (1)	P(1)-C(G11)-C(G12)	120.3 (6)	120.0 (7)
Ir(2)-C(6)-C(10)	116 (1)	113 (1)	P(1)-C(G11)-C(G16)	119.7 (5)	120.1 (6)
C(7)-C(5)-C(9)	119 (2)	121 (2)	P(1)-C(G21)-C(G22)	121.9 (5)	122.0 (5)
C(8)-C(6)-C(10)	117 (2)	121 (2)	P(1)-C(G21)-C(G26)	118.2 (5)	118.0 (4)
C(5)-C(7)-C(11)	122 (2)	122 (2)	P(2)-C(G31)-C(G32)	120.2 (6)	120.7 (7)
C(6)-C(8)-C(12)	125 (2)	124 (2)	P(2)-C(G31)-C(G36)	119.7 (5)	119.2 (5)
C(5)-C(7)-H(1)	112	119	P(2)-C(G41)-C(G42)	120.7 (6)	119.9 (5)
C(6)-C(8)-H(2)	117	119	P(2)-C(G41)-C(G46)	119.3 (5)	120.1 (4)
C(11)-C(7)-H(1)	125	120	P(3)-C(G51)-C(G52)	120.0 (6)	120.8 (5)
C(12)-C(8)-H(2)	117	117	P(3)-C(G51)-C(G56)	120.0 (5)	119.2 (5)
C(5)-C(9)-O(3)	122 (2)	127 (2)	P(3)-C(G61)-C(G62)	121.2 (6)	121.0 (5)
C(6)-C(10)-O(4)	121 (2)	121 (2)	P(3)-C(G2)-C(G66)	119.8 (5)	119.0 (5)
C(5)-C(9)-O(7)	110 (2)	110 (2)	P(4)-C(G71)-C(G72)	120.9 (6)	119.2 (6)
C(6)-C(10)-O(8)	112 (2)	116 (2)	P(4)-C(G71)-C(G76)	119.0 (6)	120.8 (5)
C(7)-C(11)-O(5)	126 (2)	130 (2)	P(4)-C(G81)-C(G82)	123.2 (6)	120.4 (5)
C(8)-C(12)-O(6)	125 (2)	128 (2)	P(4)-C(G81)-C(G86)	116.9 (5)	119.6 (5)
C(7)-C(11)-O(9)	115 (2)	110 (2)			
C(8)-C(12)-O(10)	116 (2)	112 (2)			

intensities of these bands are also consistent with this argument (see Table I); in particular, the occurrence of vibrational coupling between the mutually trans H and CO ligands results in lowering of the ν(CO) band intensity and an increase in the ν(Ir–H) intensity.[24] Attempts to confirm these assignments by preparing the deuterated analogue of **3** were unsuccessful due to our reluctance to use the large amounts of D_2 required to isolate this species as a solid. Examination of the solution IR spectra in both CH_2Cl_2 and THF also proved inconclusive due to the breadth of the bands and the appearance of additional ones arising from the complex nature of **3** in solution (vide infra). The assignment of the carbonyl bands is also consistent with those of the aforementioned alkyne adduct $[Ir_2Cl_2(CO)_2(\mu\text{-DMA})(DPM)_2]$ where ν(CO) trans to the metal–metal bond occurred at 2023 cm^{-1} while that trans to the coordinated alkyne moiety appeared at 1999 cm^{-1}.

In solution **3** displays complex behavior. At room temperature, the $^{31}P\{^1H\}$ NMR spectra show only two broad featureless peaks at ca. δ –1 and –8. When the temperature is lowered to –40 °C, the pattern sharpens into a pair of pseudotriplets at δ –1.4 and –8.6 and a small singlet at δ –5.20. Further lowering of the temperature to about –60 °C causes the downfield pseudotriplet and the singlet to collapse into the base line while the upfield pseudotriplet remains unchanged. By –100 °C a new signal has reemerged underneath the upfield signal and results in the formation of an AA′BB′ pattern centered at δ –7.6. This last pattern is very analogous to that observed for $[Ir_2Cl_2(CO)_2(\mu\text{-DMA})(DPM)_2]$ at all temperatures[8]. These observations can be explained in terms of the set of equilibria shown in Scheme I. The low-temperature limiting spectrum (–100 °C) arises from structures I and V which are identical and represent **3** as it occurs in the solid state. As the temperature is raised, chloride dissociation becomes significant allowing the equilibrium between II, III, and IV to occur. The low-temperature limiting spectrum for this equilibrium occurs at –40 °C where the equivalent structures II and IV give rise to the pair of pseudotriplets and III gives rise to the singlet. A similar equilibrium has previously been observed for $[Ir_2Cl(CO)_2(\mu\text{-DMA})(DPM)_2][BF_4]$ which was prepared by the

Scheme I

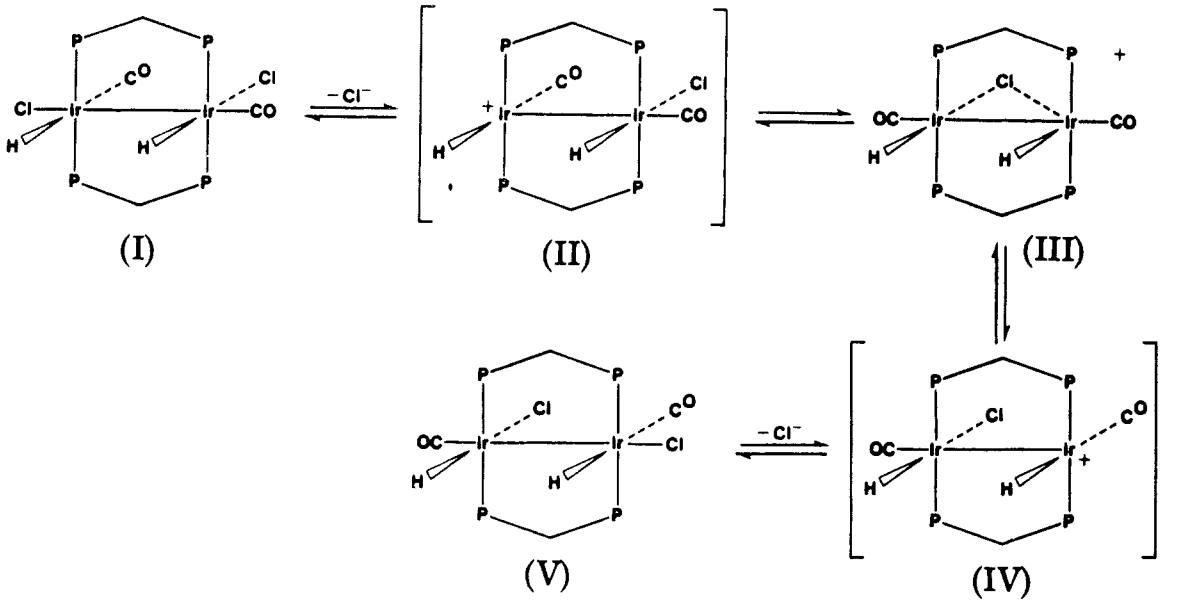

abstraction of chloride ion from $[Ir_2Cl_2(CO)_2(\mu\text{-DMA})(DPM)_2]$.[8] The ^1H NMR data also support this scheme. At room temperature only two broad peaks are observed in the hydride region. Lowering the temperature to −80 °C produces two large triplets at −5.76 and −15.10 ppm, arising from the two inequivalent hydrides in II and IV, and one small triplet at −14.86 ppm, arising from the symmetrical chloro-bridged intermediate III (see Table I). Unfortunately, the low-temperature limiting spectrum could not be obtained. Proton NMR experiments with selective ^{31}P decoupling show that the ^1H triplet at −5.76 ppm is coupled to the ^{31}P resonance at −8.6 ppm while the triplet at −15.10 ppm is coupled to the ^{31}P resonance at −1.4 ppm. Therefore, irradiating each of the two phosphorus resonances in turn causes the respective hydride resonances to collapse into a broad singlet.

Although CH_2Cl_2 solutions of **3** are nonconducting, the molar conductivity in nitromethane is only slightly less than a nomal 1:1 electrolyte, supporting the suggestion of chloride dissociation from **3**. Involvement of H_2 loss in the above fluxional process is ruled out by placing a D_2 atmosphere above solutions of **3**; no deuterium incorporation is observed over the time required to record the above spectra.

The cationic A-frame complex $[Ir_2(CO)_2(\mu\text{-Cl})(DPM)_2][BF_4]$, **2**, also reacts rapidly with hydrogen to give a very pale yellow solution containing a single species **4**. The ^1H NMR spectrum indicates that **4** is a tetrahydride species resulting from the coordination of two molecules of hydrogen to **2** (see Table I). The ^1H and ^{31}P NMR spectra also indicate that **4** is fluxional in solution. The low-temperature limiting ^1H spectrum shows four distinct terminal hydride resonances, three of which broaden and collapse into the base line as the temperature is raised while the fourth resonance, that which is most upfield, remains sharp. No limiting spectrum could be obtained in the $^{31}P\{^1H\}$ NMR spectra, but the room-temperature spectrum displays an AA′BB′ pattern, suggesting that the time-averaged geometry of **4** is unsymmetrical. Placing D_2 above solutions of **4** has no affect on the ^1H NMR spectrum after 15 min ruling out H_2 loss as a step in the fluxional process. It is not clear from this information what the structure of **4** is or what processes are involved in the fluxional behavior.

When a solution of **4** is refluxed in THF for 20 min, a new species, **5**, is formed in quantitative yield. The ^1H NMR and IR spectra indicate that this species is a dicarbonyl dihydride species formed by the loss of one molecule of H_2 from **4**, and adding H_2 to a solution of **5** readily regenerates **4**. On the basis of the above data and the $^{31}P\{^1H\}$ spectra which show a symmetrical species over all temperatures, there are two possible structures for **5** which are difficult to distinguish by spectroscopy alone. These structures are shown as VI and VII. Structure VI

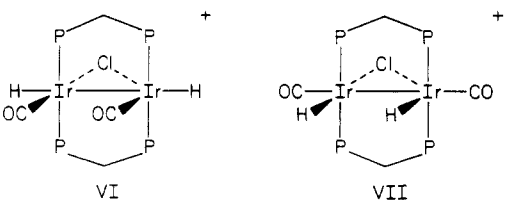

appears to be correct based on the observation that prolonged refluxing of solutions of **5** fails to result in any H_2 loss, suggesting that the hydrides are not mutually cis. Structure VI is also consistent with the X-ray structure of the alkyne-inserted product **7** (vide infra). It is significant that the symmetrical species observed in CH_2Cl_2 solutions of **3**, and proposed to have a structure related to VII, has rather different spectral parameters from those of **5**; this again suggests that **5** has structure VI. That species having structures VI and VII should have different spectral parameters is totally expected since for the former the carbonyl groups are pseudo-trans to the bridging chloro group, whereas for the latter it is the hydrides which are opposite the Cl ligand. Compound **5** can also be prepared by the reaction of **3** with $AgBF_4$, suggesting that chloride abstraction is accompanied by a rearrangement. Since complexes **5** and **4** are related by the respective gain and loss of H_2, some ligand rearrangement must have occurred in the initial formation of **4** from the reaction of **2** with H_2 if VI is the correct structure for **5**. Simple addition of 2 equiv of H_2 to **2** without some rearrangement cannot produce a species which would generate **5** (having structure VI) upon H_2 loss.

Compound **3** reacts quantitatively with 1 equiv of DMA to give rise to a new product, $[Ir_2HCl_2(CH_3O_2CC{=}CHCO_2CH_3)(CO)_2(DPM)_2]$ (**6**). The ^1H NMR spectrum of **6** shows one hydride resonance at δ −8.89 and a singlet at δ 3.85, each integrating as one hydrogen (see Table I). Similarly, the IR spectrum shows only one ν(Ir—H) band in addition to new ν(C=O) and ν(C=C) bands of the DMA

Scheme II

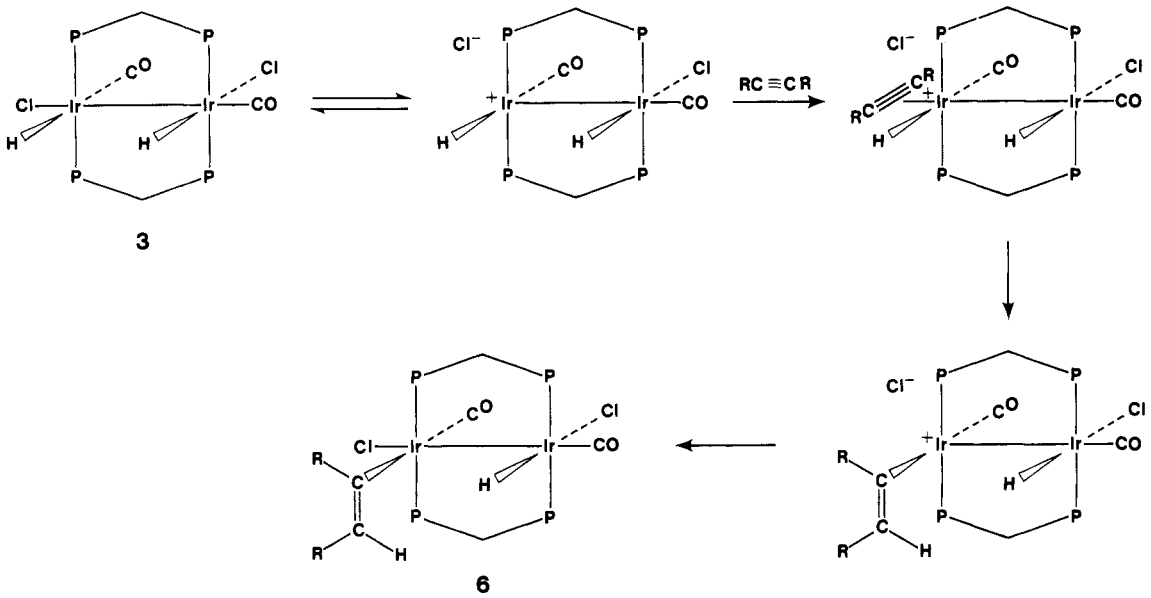

3 6

ligand. This spectroscopic information, coupled with the observation of a $^{31}P\{^1H\}$ pattern typical of an unsymmetrical species, suggests the structure shown below for **6** in which the alkyne has inserted into one of the Ir–H bonds of **3**. Although compound **3** is coordinatively saturated in the solid state and so would not be expected to react further, Cl^- dissociation from one iridium center occurs in solution yielding the unsaturated cationic intermediate II, as pointed out earlier in Scheme I. Coordination of the alkyne at this metal, followed by insertion into the Ir–H bond and Cl^- recoordination, would yield **6** as shown in Scheme II.

Attempts to induce further reaction between the metalated olefin and the remaining hydride ligand have been unsuccessful. In order for further reaction to occur, it is apparent that an open coordination site and the concomitant coordinative unsaturation must be generated at the metal having the hydride ligand, either by loss of chloride ion or carbon monoxide. However, the removal of chloride ion by the reaction of **6** with $AgBF_4$ does not proceed as suggested but leads only to the isolation of **7** (vide infra) in low yield (<30% after workup). The formation of **7** from **6** indicates that at some point alkyne loss, rearrangement, and subsequent alkyne insertion into the second Ir–H bond has occurred. The alternative method of producing an open coordination site, involving removal of a carbonyl group from **6**, has also proven unsuccessful; refluxing **6** in CH_2Cl_2 for 2 h had no effect. Other means of CO removal are now under investigation. It may be possible that insertion of the metalloolefin moiety into the second Ir–H bond is inhibited by steric interactions involving the metalated olefin and DPM phenyl rings. Attempts to obtain suitable crystals of **6** in order to determine its X-ray structure have been unsuccessful to date.

Compound **5** also reacts with DMA. However in contrast to compound **3**, at least a twofold excess must be used and the reaction does not proceed to one product. Within 16 h after the reaction is initiated, the $^{31}P\{^1H\}$ NMR spectrum shows that **5** has been completely consumed and three new species have been formed. This NMR spectrum consists of a complex multiplet (δ −12.5, −16.5) and two singlets (at δ −13.6, −17.6) in the approximate ratio 4.5:2.1:1.0. A ^1H NMR spectrum of this mixture shows no hydride resonances while the region from 3 to 6 ppm is very complex. An IR spectrum of the solid mixture shows carbonyl bands at 2019, 2024, 1987, and 1947 cm^{-1} and a broad BF_4^- band at 1050 cm^{-1}. By means of column chromatography, the major species of the mixture, $[Ir_2Cl_2(CH_3O_2CC{=}CHCO_2CH_3)_2(CO)_2(DPM)_2]$ (**7**), was separated in ca. 50% yield. ^1H NMR and IR spectra indicate that **7** is a di-inserted product which no longer contains BF_4^-. This is confirmed by elemental analysis and an X-ray structure determination which showed it to have the geometry as in Figure 1. Although **7** is symmetrical in the solid state, in solution the ends of the dimer are no longer equivalent as evidenced by the ^1H and $^{31}P\{^1H\}$ NMR spectra. Compound **7** is not an electrolyte, even in nitromethane, so chloride ion dissociation cannot be responsible for the solution asymmetry; instead some other distortion of the complex must occur in order to relieve some of the steric crowding in the molecule.

Complex **7** is isolated as a neutral dichloride whereas the parent compound **5** is a cationic monochloride, posing a question as to the source of the second chloride ion. The source appears to be the CH_2Cl_2 solvent rather than disproportion of the cationic precursor, since **7** is observed to form in greater than 50% yield in the initial reaction mixture. Further evidence comes from the observation that the reaction does not proceed by an identical route when performed in acetone.[25] The reaction likely proceeds by the initial formation of a cationic di-inserted species $[Ir_2(CH_3O_2CC{=}CHCO_2CH_3)_2(CO)_2(\mu\text{-}Cl)(DPM)_2][BF_4]$ which subsequently abstracts chloride ion from the solvent. It is possible that it is this complex which gives rise to one of the singlets observed in the $^{31}P\{^1H\}$ NMR spectrum of the original reaction mixture. Further studies using solvents other than CH_2Cl_2 are underway at the present time.

Attempts to react compound **7** with H_2 in order to complete a hydrogenation cycle have failed; however, on the basis of the coordinative saturation at both metals, this is not surprising.

Conclusions

The binuclear complexes *trans*-$[IrCl(CO)(DPM)]_2$ (**1**) and $[Ir_2(CO)_2(\mu\text{-}Cl)(DPM)_2][BF_4]$ (**2**) have been shown to react rapidly with hydrogen under mild conditions. The reaction of **2** initially produces a tetrahydride species which can be converted into a dihydride upon refluxing under N_2. This latter species reacts with excess DMA to give a

(25) Cowie, M.; Sutherland, B. R.; Vaartstra, B. A., unpublished results.

product in which alkyne insertion into each Ir-H bond has occurred. It is not clear how this relates (if at all) to the catalytic hydrogenation of alkynes by the rhodium analogue, $[Rh_2(CO)_2(\mu\text{-}Cl)(DPM)_2]^+$, although further studies are currently underway to investigate this possibility. It may also be that it is the initial tetrahydride species **4** which is analogous to the catalytically important species in the rhodium-catalyzed cycle and further studies are currently underway in attempts to characterize this tetrahydride species and to investigate its subsequent chemistry with unsaturated substrates.

In contrast, the reaction of **1** with H_2 produces a dihydride species which subsequently reacts with only 1 equiv of DMA. Spectroscopic evidence shows that the alkyne has inserted into only one of the Ir-H bonds. Although this insertion occurs at only one metal center, we can forsee how the second metal can become involved through π-coordination of the metalated olefin moiety to the second metal and subsequent hydrogen transfer to the olefin to form a dimetalated alkyl group which then reductively eliminates as the olefin. Attempts to induce the second hydrogen transfer and subsequent reductive elimination have not yet met with sucess in the complex studied. It is not clear whether this is due to the steric bulk of the phosphine and alkyne groups or whether it is a function of the low lability of the chloro or carbon monoxide ligands, failing to generate the required coordinative unsaturation. Attempts to react this single alkyne-inserted product (**6**) with H_2 under ambient conditions have also been unsuccessful. Further studies are underway in attempts to react **6** further and to determine the reasons for the apparent lack of reactivity under the conditions studied.

The reason that the neutral compound **3** reacts with only 1 equiv of alkyne whereas the cationic species **5** reacts with 2 equiv seems to be due to "incipient coordinative unsaturation" in the latter; the coordinative unsaturation required for alkyne coordination at each metal center in turn can be generated in **5** by movement of the halide ligand from the bridging position to a terminal site on the opposite metal. This transfer of the halide ligand back and forth between the metals, generating coordinative unsaturation, shows one way in which adjacent metal centers can cooperate in catalysis.

Acknowledgment. This work was supported by the University of Alberta and the Natural Sciences and Engineering Research Council of Canada. We thank NSERC for a scholarship to B.R.S. and for partial funding of the diffractometer through a grant to M.C. and acknowledge Mr. Brian A. Vaartstra for technical assistance.

Registry No. 1, 66125-35-7; 2, 90552-98-0; 3, 97690-03-4; 4, 97690-05-6; 5, 97690-07-8; 6, 97690-08-9; 7, 97690-09-0; DMA, 762-42-5; Ir, 7439-88-5.

Supplementary Material Available: Listing of observed and calculated structure factors, thermal parameters for the anisotropic atoms, and idealized hydrogen parameters (36 pages). Ordering information is given on any current masthead page.

Tantalum Organometallics Containing Bulky Oxy Donors: Utilization of Tri-*tert*-butylsiloxide and 9-Oxytriptycene

Robert E. LaPointe, Peter T. Wolczanski,* and Gregory D. Van Duyne

Department of Chemistry, Baker Laboratory, Cornell University, Ithaca, New York 14853

Received January 31, 1985

Procedures entailing the preparation of alkyl- and chlorotantalum complexes containing 9-oxytriptycene (TpO) and $(t\text{-}Bu)_3SiO^-$ (silox) are described. Addition of 2 equiv of $TpOSiMe_3$ to $TaCl_5$ yielded $(TpO)_2TaCl_3$ (**2**); alcoholysis of $Np_3Ta{=}C(H)CMe_3$ (Np = neopentyl) with TpOH produced $(TpO)_2TaNp_3$ (**3**). An X-ray structure determination of **3** indicated that the axially disposed TpO units are nearly eclipsed in this pseudo-tbp complex. Crystal data: orthorhombic, $Pn2_1a$, a = 16.024 (2) Å, b = 13.607 (4) Å, c = 21.377 (1) Å, Z = 4, and T = 25 °C. From 2651 data were $|F_o| \geq 3\sigma(|F_o|)$, an R factor of 0.054 was obtained via standard refinement methods. Short Ta-O bonds (1.869 (16) Å average) concomitant with near linear Ta-O-C angles (170.3 (19) and 163.9 (16)°) suggest that strong π-bonding is evident. Treatment of $TaCl_5$ and R_3TaCl_2 (R = Me, CH_2Ph, Np) with stoichiometric amounts of Na(silox) gave $(silox)_2TaCl_3$ (**4**), $(silox)_2TaR_3$ (R = Me (**5**), CH_2Ph (**6**)), $(silox)_2NpTa{=}C(H)CMe_3$ (**11**), and $(silox)TaNp_3Cl$ (**9**), respectively. From Np_2TaCl_3 and 2Na(silox), $(silox)_2TaNp_2Cl$ (**10**) was obtained. Either **9** and Na(silox) or **10** and NpLi also afforded **11**. Thermolysis of **6** provided $(silox)_2Ta{=}C(H)Ph(CH_2Ph)$ (**7**), and the addition of $PhCH_2MgCl$ to **4** in Et_2O resulted in $(silox)_2TaCl_2(CH_2Ph)$ (**8**). $Np_3Ta{=}C(H)CMe_3$ reacted with (silox)H to form $(silox)Np_2Ta{=}C(H)CMe_3$ (**12**), but further silanolysis was not observed. Discussions pertaining to the effective size of the oxygen donor ligands, the stability of the complexes, and their relationship to analogous Cp species are presented.

Introduction

The generation of organotransition-metal complexes possessing a degree of coordinative unsaturation remains a critical problem in regard to the catalytic and stoichiometric transformations of small molecules.[1] In this regard, the approach of sterically saturating a metal center, which can remain electronically deficient, may be a plausible

(1) Parshall, G. W. "Homogeneous Catalysis"; Wiley-Interscience: New York, 1980.

0276-7333/85/2304-1810$01.50/0 © 1985 American Chemical Society